The Effects of Aperture Jitter and Clock Jitter in Wideband ADCs

Michael Löhning and Gerhard Fettweis
Dresden University of Technology
Vodafone Chair Mobile Communications Systems
D-01062 Dresden, Germany
e-mail: loehning@ifn.et.tu-dresden.de

Abstract

Designing leading-edge systems (e.g., communications systems) requires knowledge about the technological limits. Jitter is the limiting effect in ADCs with a digitization bandwidth between 1 MHz and 1 GHz. The effect of aperture jitter and clock jitter have been investigated previously. However, some very important aspects are still missing, in particular investigations on the spectral distribution of the jitter induced error. This gap is filled by this paper.
Keywords: wideband ADC, aperture jitter, clock jitter, signal-to-noise ratio, error spectrum

1 Introduction

Modern mobile communication receivers require high speed analog-to-digital converters which provide a high resolution for a wide digitization bandwidth. This is particularly true for reconfigurable multimode receivers. Due to technology dependent physical error effects today's state-of-the-art wideband ADCs cannot cope with the enormous requirements regarding resolution, speed, and digitization bandwidth in such receivers. In [1] *Walden* identified the aperture jitter as the dominating error effect that limits the achievable signal-to-noise ratio (SNR) and therefore the resolution of wideband ADCs (with digitization bandwidths between 1 MHz and 1 GHz). As will be clarified in the paper, clock jitter influences the achievable SNR in a similar way.

In the last few years different authors derived formulas to quantify the SNR limiting effect of jitter in ADCs. While *Walden* used a worst case approach [1], *Kobayashi* presented an exact formula which allows to calculate the SNR in the presence of an aperture jitter [2]. The effect of the clock jitter was investigated by *Awad* [3], but only for the special case of sinusoidal input signals.

This paper presents an explicit analysis of both the aperture jitter and the clock jitter effect for arbitrary stationary input signals. Additionally to the SNR formulas, also expressions for the corresponding error spectra at the ADC output are derived. The presented results enable developers of new receiver concepts to decide if and by which means jitter effects in the ADC can be compensated. Further they are useful for designers of future air interfaces (e.g. 250 Mbit/s WLAN) who have to consider theoretical limits of ADC resolution and digitization bandwidth determined by the jitter parameters of current or future technologies.

This work is a contribution to the project RMS (Reconfigurable Mobile Communication Systems) funded by the German Ministry for Education and Research (BMBF) and by the Alcatel SEL AG, Stuttgart, Germany.

2 Sampling with jitter

Consider a real periodic ADC input signal given by its Fourier series expansion

$$s(t) = c_0 + \sum_{k=1}^{\infty}\Big[\underbrace{c_k\, e^{-j\varphi_k}}_{\underline{c}_{-k}}\, e^{-j2\pi f_k t} + \underbrace{c_k\, e^{j\varphi_k}}_{\underline{c}_k}\, e^{j2\pi f_k t}\Big] \qquad (1)$$

In order to obtain general results independent of a special (possibly unknown) phase spectrum, the phases φ_k shall be assumed as independent random variables uniformly distributed in the range $(-\pi, \pi)$. With this assumption (1) can be written in the form

$$s(t) = \sum_{i=-\infty}^{\infty} \underbrace{\underline{c}_i\, e^{j2\pi f_i t}}_{s_i(t)} \quad \text{with} \quad \mathrm{E}\{\underline{c}_i \underline{c}_k^*\} = \begin{cases} |\underline{c}_i|^2 & \text{if } i = k \\ 0 & \text{else} \end{cases} \qquad (2)$$

which describes a wide-sense stationary (WSS) random process with the complex components $s_i(t)$ [4].

In the ADC $s(t)$ is sampled at the time instants $t_n = nT + J_n$ with the nominal sampling period T. J_n are the random sampling time variations due to aperture and clock jitter. For a block of N sampling points the mean error power caused by the random jitter process can be calculated as

$$P_J = \frac{1}{N}\sum_{n=0}^{N-1} \mathrm{E}\{e(nT)e^*(nT)\}$$

where

$$e(nT) = s(nT+J_n) - s(nT) = \sum_{i=-\infty}^{\infty} \underbrace{s_i(nT+J_n) - s_i(nT)}_{e_i(nT)}$$

stands for the n-th error sample. As one can show, using the orthogonality property of the signal components $s_i(t)$ (see (2)), the sampling errors $e_i(nT)$ generated for different signal components are as well orthogonal, i.e. the corresponding error powers accumulate:

$$P_J = \frac{1}{N}\sum_{n=0}^{N-1}\sum_{i=-\infty}^{\infty} \mathrm{E}\left\{|e_i(nT)|^2\right\} \qquad (3)$$

The derivation of the mean sampling error power $\mathrm{E}\left\{|e_i(nT)|^2\right\}$ caused by jitter for a single complex signal component $s_i(t)$ is straightforward. Using the relationship

$\mathrm{E}\{e^{j\mu J_n}\} = \mathrm{E}\{e^{-j\mu J_n}\}$, which holds for every zero mean jitter process with symmetrical probability density functions (pdfs), one gets

$$\mathrm{E}\{|e_i(nT)|^2\} = 2\,|\underline{c}_i|^2\left(1 - \mathrm{E}\{e^{j2\pi f_i J_n}\}\right)$$

and finally

$$P_J = \frac{1}{N}\sum_{n=0}^{N-1}\sum_{i=-\infty}^{\infty} 2\,|\underline{c}_i|^2\left(1 - \mathrm{E}\{e^{j2\pi f_i J_n}\}\right) \quad (4)$$

where $\mathrm{E}\{e^{j2\pi f_i J_n}\}$ is the characteristic function of the overall jitter process.

So far only periodic input signals have been considered. The results can easily be extended to non-periodic signals. Substituting the definition of the Fourier coefficients $c_i = \frac{1}{T_0}\int_{-T_0/2}^{T_0/2} s(t)e^{j2\pi i f_0 t}$ (with the signal period $T_0 = f_0^{-1}$ and $f_i = i f_0$) into (4) and taking the limit for $T_0 \to \infty$ yields

$$P_J = \frac{1}{N}\sum_{n=0}^{N-1} 2\int_{-\infty}^{\infty} S_{ss}(f)\left(1 - \mathrm{E}\{e^{j2\pi f J_n}\}\right)df$$

where $S_{ss}(f)$ is the power spectral density (psd) of $s(t)$. Finally, the jitter dependent SNR (in decibels) is given by

$$SNR_J = 10\lg\left(\frac{\int_{-\infty}^{\infty} S_{ss}(f)df}{\frac{2}{N}\sum\limits_{n=0}^{N-1}\int\limits_{-\infty}^{\infty} S_{ss}(f)\left(1 - \mathrm{E}\{e^{j2\pi f J_n}\}\right)df}\right)\mathrm{dB} \quad (5)$$

Not only the mean sampling error power has to be considered for a complete description of the effects of aperture jitter and clock jitter in ADCs, but also its spectral distribution, i.e. the corresponding error power spectrum $S_{ee}(e^{j2\pi fT})$ at the ADC output. $S_{ee}(e^{j2\pi fT})$ is defined as the discrete-time Fourier transform (DTFT) of the error auto-correlation function $s_{ee}(nT, mT) = \mathrm{E}\{e(nT)e^*(mT)\}$. Using the stochastic input signal model described by (2), the following expression can be derived for the error auto-correlation function at the ADC output.

$$s_{ee}(nT, mT) = \sum_{i=-\infty}^{\infty} |\underline{c}_i|^2 e^{j2\pi f_i(n-m)T}\cdot\Big[1 + \mathrm{E}\{e^{j2\pi f_i(J_n - J_m)}\} - \mathrm{E}\{e^{j2\pi f_i J_n}\} - \mathrm{E}\{e^{-j2\pi f_i J_m}\}\Big] \quad (6)$$

As can be seen, the error auto-correlation function depends on the characteristic functions $\mathrm{E}\{e^{j2\pi f J_n}\}$ and $\mathrm{E}\{e^{-j2\pi f J_m}\}$ of the overall jitter process at the sampling time instants nT, mT and of the characteristic function $\mathrm{E}\{e^{j2\pi f(J_n - J_m)}\}$ of the difference $J_n - J_m$. Before transforming (6), i.e. calculating the corresponding error power spectrum, it is useful to analyze $\mathrm{E}\{e^{j2\pi f J_n}\}$, $\mathrm{E}\{e^{-j2\pi f J_m}\}$, and $\mathrm{E}\{e^{j2\pi f(J_n - J_m)}\}$ for the different kinds of jitter. This will be done in the next section.

3 Jitter models

Aperture jitter stands for the random sampling time variations in ADCs which are caused by thermal noise in the sample-&-hold circuit. It is commonly modeled as independent Gaussian jitter [3], i.e. the corresponding sampling time variations $J_n^{ap} = t_n - nT$ are assumed to be independent identically distributed (i.i.d.) Gaussian random variables with zero mean and the variance σ_{ap}^2. Hence, the following equations hold

$$\mathrm{E}\{e^{\pm j2\pi f J_n^{ap}}\} = \mathrm{E}\{e^{\pm j2\pi f J_m^{ap}}\} = e^{-2\pi^2 f^2 \sigma_{ap}^2} \quad (7)$$

and

$$\mathrm{E}\{e^{j2\pi f(J_n^{ap} - J_m^{ap})}\} = \begin{cases} 1 & \text{if } n = m \\ \left[e^{-2\pi^2 f^2\sigma_{ap}^2}\right]^2 & \text{if } n \neq m \end{cases} \quad (8)$$

Clock jitter is a property of the clock generator that feeds the ADC with the clock signal. It is caused by the phase noise of the oscillator and generates additional sampling time errors in the ADC. In [5] is shown that the phase noise of free running oscillators can be modeled as a Wiener process, i.e. a continuous-time non-stationary random process with independent Gaussian increments. Time-discretization of the Wiener process yields the model of accumulated timing-jitter commonly used for clock jitter [3], where the sampling time variations J_n^{acc} are modeled as

$$J_0^{acc} \doteq 0 \qquad \text{and} \qquad J_n^{acc} = \sum_{i=1}^{n} \delta_i$$

The jitter increments δ_i are i.i.d. Gaussian random variables with zero mean and the variance $\sigma_{\delta_i}^2 = cT$. The product cT of the phase noise constant c of the oscillator and the nominal clock period T is a typical parameter of clock generators known as cycle-to-cycle jitter variance. Using the accumulated jitter model the following expressions for the characteristic jitter functions can be derived

$$\mathrm{E}\{e^{\pm j2\pi f J_n^{acc}}\} = \left[\mathrm{E}\{e^{j2\pi f\delta_1}\}\right]^n = e^{-2\pi^2 f^2 cnT} \quad (9)$$

and

$$\mathrm{E}\{e^{j2\pi f(J_n^{acc} - J_m^{acc})}\} = e^{-2\pi^2 f^2 cT|n-m|} \quad (10)$$

It should be noted that in the case of clock jitter the characteristic functions depend on the absolute sampling time while in the case of aperture jitter they are time-invariant.

4 Aperture jitter versus clock jitter effects

By means of the jitter models presented in section 3 the error effects caused by aperture and by clock jitter shall be compared. The overall SNR as well as the spectral distribution of the mean error power will be considered.

Comparison of the overall SNR

Substituting the characteristic jitter functions given by (7) and (9) into (5) yields the following SNR formulas

$$SNR_{ap} = 10\lg\left(\frac{\int_{-\infty}^{\infty} S_{ss}(f)df}{2\int\limits_{-\infty}^{\infty} S_{ss}(f)\left(1 - e^{-2\pi^2 f^2\sigma_{ap}^2}\right)df}\right)\mathrm{dB}$$

$$SNR_{acc} = 10\lg\left(\frac{\int_{-\infty}^{\infty} S_{ss}(f)df}{\frac{2}{N}\sum_{n=0}^{N-1}\int_{-\infty}^{\infty} S_{ss}(f)\left(1 - e^{-2\pi^2 f^2 cnT}\right)df}\right)\mathrm{dB}$$

As can be seen, in the case of aperture jitter the signal-to-noise ratio is independent of the number of sampling points N (and therefore of the sampling block length NT), while in the case of clock jitter the SNR strongly depends on it. This fact is illustrated by the curves in Fig. 1, which show the corresponding SNRs calculated for different sampling block lengths assuming a 50 MHz sine wave as an input signal, a sampling frequency of 100 MHz, and the given jitter parameters.

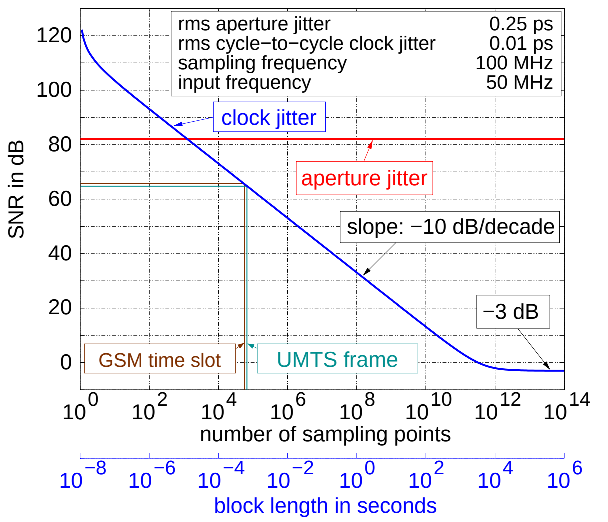

Figure 1: Comparison of the mean SNR caused by aperture and clock jitter while sampling a 50 MHz sine wave using different sampling block lengths

In Fig. 2 the SNR formulas are evaluated for a fixed sampling block length of 1 ms. The sampling frequency and the jitter parameters are the same as in Fig. 1. The solid curves represent the results for a sinusoidal input signal with the specified frequencies. The dashed curves are calculated for a band-limited white noise input with different cut-off frequencies. One can see that the SNR trends are, in principle, the same for both kinds of jitter as well as for both kinds of input signals. The SNR decreases with about 6 dB per doubling the input frequency or bandwidth (which is equivalent to a loss of 1bit of ADC resolution) and converges to −3 dB if the highest input frequency exceeds the inverse rms (root mean square) jitter values σ_{ap}^{-1} and $1/\sqrt{cNT}$. The following can be concluded:

1. The SNR is mainly determined by the highest frequency components of the input signal and secondarily by its bandwidth.

2. Although the absolute SNR values strongly depend on the jitter parameters of the ADC and the clock generator in connection with the specific sampling block length, the effect of aperture and clock jitter on the overall SNR is, in principle, the same.

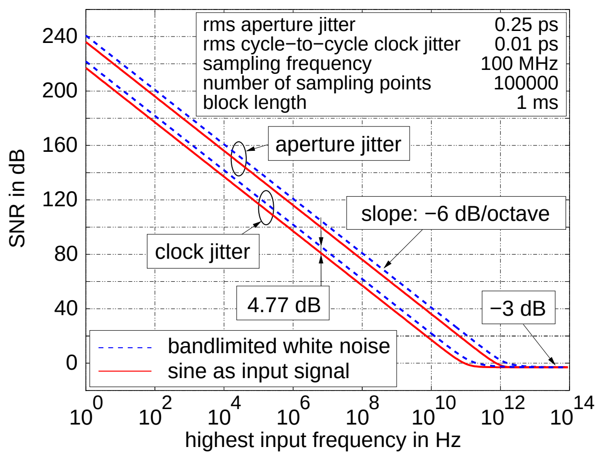

Figure 2: Comparison of the SNR caused by aperture and clock jitter for a sinusoidal input signal and a bandlimited white noise input with different signal/cut-off frequencies

Comparison of the error power spectra

In order to obtain expressions for the error power spectra caused by the different jitter processes, the corresponding error auto-correlation functions s_{eeap} and s_{eeacc} will be derived and transformed by means of the DTFT.
Using the definition $k = n - m$ and substituting (7) and (8) into (6) yields the error auto-correlation function for the case of **aperture jitter**

$$s_{eeap}(kT) = \underbrace{\sum_{i=-\infty}^{\infty} |\underline{c}_i|^2 e^{j2\pi f_i kT} \cdot g_i^2}_{\text{periodic part}} + \underbrace{|\underline{c}_i|^2 \cdot [2g_i - g_i^2] \cdot \delta_{Kr}(k)}_{\text{aperiodic part}}$$

Here $g_i = \left(1 - e^{-2\pi^2 f_i^2 \sigma_{ap}^2}\right)$ denotes a gain coefficient specific for each spectral component of the input signal and $\delta_{Kr}(k) = \begin{cases} 1 & \text{if} \quad k = 0 \\ 0 & \text{else} \end{cases}$ stands for the Kronecker impulse.
By transforming $s_{eeap}(kT)$ to the frequency domain one gets

$$S_{eeap}\left(e^{j2\pi fT}\right) = \quad (11)$$
$$\underbrace{\frac{1}{T}\sum_{l=-\infty}^{\infty}\sum_{i=-\infty}^{\infty} |\underline{c}_i|^2 \delta\left(f - f_i - \frac{l}{T}\right) \cdot g_i^2}_{\text{periodic line spectrum}} + \underbrace{\sum_{i=-\infty}^{\infty} |\underline{c}_i|^2 \cdot [2g_i - g_i^2]}_{\text{constant}}$$

The resulting error power spectrum consists of a constant term and a term comprising the spectral components of the input psd weighted with the squares of the spectral gains g_i. In the majority of applications the maximum input signal frequency $f_{i_{max}}$ is very low compared to the inverse of the rms jitter value σ_{ap}. Hence, the gains g_i get very small so that the error power spectrum can be approximated by

$$S_{eeap}\left(e^{j2\pi fT}\right) \approx \sum_{i=-\infty}^{\infty} 2|\underline{c}_i|^2 \cdot g_i = \text{const} \quad (12)$$

Eq. (12) proves the common assumption that the mean error power caused by aperture jitter (in most cases) is equally distributed over the whole digitization band ($-1/2T < f < 1/2T$), which motivates the approach to increase the jitter dependent SNR in a given frequency band by means of oversampling and filtering.

For the case of **clock jitter** the following error autocorrelation function can be derived

$$s_{eeacc}(kT, nT) = \sum_{i=-\infty}^{\infty} |\underline{c}_i|^2\, e^{j2\pi f_i kT}\Big[1 + e^{-2\pi^2 f_i^2 c|k|T} - e^{-2\pi^2 f_i^2 cnT} - e^{-2\pi^2 f_i^2 c\overbrace{(n-k)}^{m}T}\Big] \quad (13)$$

In contrast to the aperture jitter case s_{ee} does not only depend on the sampling time difference $kT = (n-m)T$ but also on the absolute sampling time instants. Only for $n \to \infty$, when the last two terms in (13) vanish, s_{eeacc} becomes independent of n and m and can be discrete-time Fourier transformed in the common way, resulting in

$$S_{eeacc}\big(e^{j2\pi fT}, nT\big)\Big|_{n\to\infty} = \frac{1}{T}\sum_{l=-\infty}^{\infty} \delta\Big(f - \frac{l}{T}\Big) * \Big[\sum_{i=-\infty}^{\infty} |\underline{c}_i|^2\, \delta(f - f_i) + |\underline{c}_i|^2 \underbrace{\frac{f_i^2 c}{\pi^2 f_i^4 c^2 - (f - f_i)^2}}_{\text{Lorentzian spectrum}}\Big] \quad (14)$$

where $*$ denotes the convolution operator. In this case the error power spectrum consists of the spectral components of the input psd, each overlayed by a Lorentzian spectrum. In practical applications the sampling block length is limited ($n < \infty$). In order to model the error power spectrum in this case one can use the following approach. For each sampling time instant nT a short time error power spectrum is calculated. The observation period is determined by the sampling block length NT, which should not be to small in order to reduce windowing effects. The resulting spectra can be interpreted as a time-varying power spectrum $S_{eeacc}\big(e^{j2\pi fT}, nT\big)$ in the sense of a (modified) Rihaczek spectrum [6]. Hence, the time average

$$\overline{S}_{eeacc}\big(e^{j2\pi fT}\big) = \frac{1}{N}\sum_{n=0}^{N-1} S_{eeacc}\big(e^{j2\pi fT}, nT\big) \quad (15)$$

is supposed to be a meaningful measure of the spectral distribution of the mean error power. Numerical evaluations of (15) show that for sufficient small rms clock jitter values ($\sqrt{cNT} \ll f_{i_{max}}^{-1}$) the error power caused by accumulated clock jitter is strongly concentrated around the frequency components of the input signal. Moreover, the partial frequency-dependent error power (see also Fig. 2) generated by a certain spectral component of the input signal is concentrated around this very component. As a general difference to the aperture jitter effect it can be concluded that the error noise caused by clock jitter is highly correlated. Consequently, the jitter dependent SNR cannot be increased by oversampling techniques.

5 Simulation results

In order to confirm the results derived above, some simulation results are presented.

Fig. 3 shows the error power spectrum simulated for an input signal that comprises two equal-power sine waves with the frequencies of 10 MHz and 100 MHz. The overall input signal power was normalized to one. The signal was sampled with a sampling frequency of 400 MHz and white Gaussian aperture jitter with a standard deviation of 0.25 ps. As predicted by the analytical results for $f_{i_{max}} \ll \sigma_{ap}^{-1}$, the error power spectrum is white.

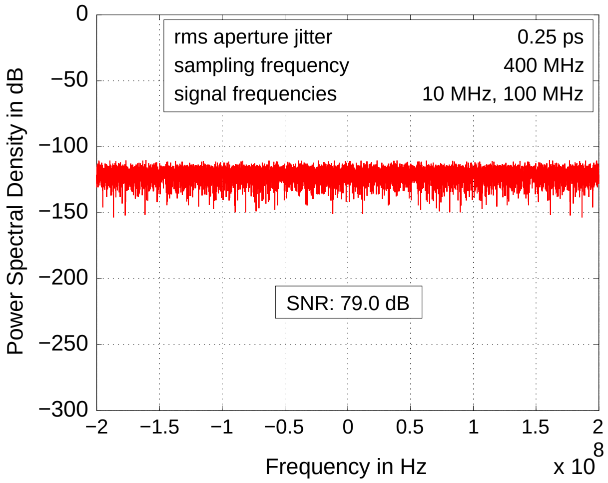

Figure 3: Mean error psd caused by **aperture jitter** while sampling a mix of two equal power sine waves whose frequencies are **very low** compared to the inverse rms jitter value

To obtain the error power spectrum in Fig. 4 the same input signal was used. Now it was sampled with accumulated Gaussian clock jitter. The sketched error psd is the average of 100 independent Monte Carlo simulations. The chosen phase noise constant and the sampling block length ensure that the condition $f_{i_{max}} \ll 1/\sqrt{cNT}$ holds. As expected, the error power spectrum shows narrow peaks at ±10 MHz and ±100 MHz. The fact, that the peak psd values differ, confirms the statement that the partial frequency-dependent error power generated for a certain signal component $\underline{c}_i e^{j2\pi f_i t}$ concentrates around the corresponding frequency f_i. The lower the frequency of the error-generating signal component, the lower is the corresponding error power.

Figs. 5 and 6 show the error power spectra generated by aperture jitter and clock jitter for a sine wave input signal whose frequency equals σ_{ap}^{-1} or exceeds $1/\sqrt{cNT}$, respectively. The signal amplitude was normalized to one. In the aperture jitter case the error psd comprises the typical white noise floor and in addition the two spectral lines of the input psd. This corresponds to the theoretically derived expression in (11). The error psd in Fig. 6 generated

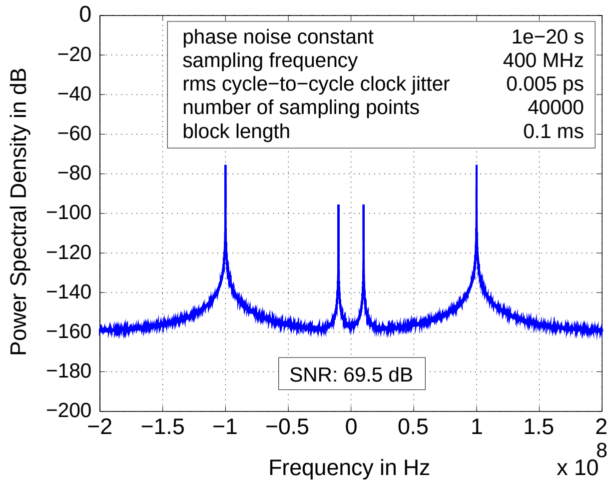

Figure 4: Mean error psd caused by **clock jitter** while sampling a mix of two equal-power sine waves whose frequencies are **very low** compared to the inverse rms jitter value $1/\sqrt{cNT}$

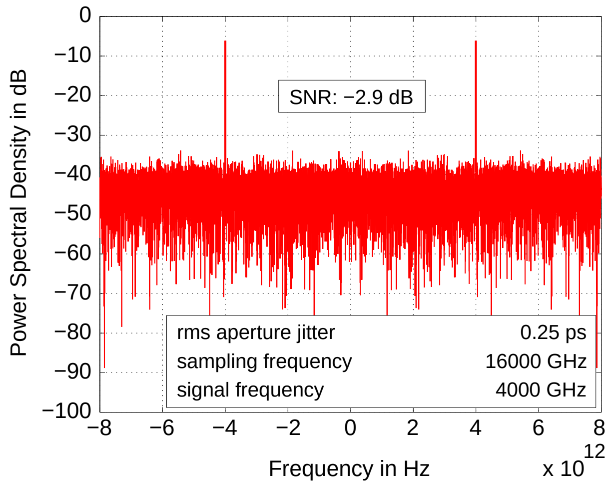

Figure 5: Mean error psd caused by **aperture jitter** while sampling a sine wave whose frequency **equals** the inverse rms jitter value

by clock jitter for a large number of sampling points is similar to that determined by (14).
Finally, it should be noted that the simulated SNR values are in accordance with the analytically predicted results.

6 Conclusions

The similarities and differences of the error effects caused by aperture and clock jitter in wideband ADCs have been presented. As an extension to previous publications not only the overall SNR was considered but also the spectral distribution of the generated error power. By means of analytically derived expressions (confirmed by simulations) it has been shown that the SNR limiting effect of aperture jitter and clock jitter is, in principle, the same, but the resulting error power spectra are significantly different. In the case of aperture jitter the mean error power

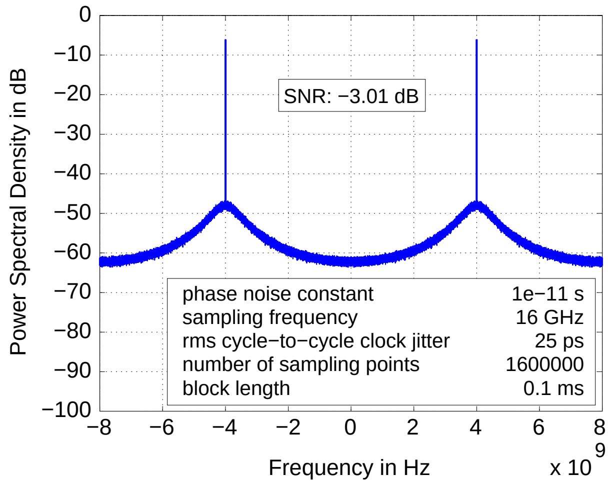

Figure 6: Mean error psd caused by **clock jitter** while sampling a sine waves whose frequency **is greater** than the inverse rms jitter value $1/\sqrt{cNT}$

is uniformly distributed over the whole digitization band, so that the jitter dependent SNR in a given frequency band can be increased by oversampling techniques. In the case of clock jitter the error power is concentrated around the frequencies of the input signal components. Thus, oversampling does not help to increase the SNR.

References

[1] R. H. Walden, “Analog-to-Digital Converter Survey and Analysis,” *IEEE J. Select. Areas Commun.*, vol. 17, no. 4, pp. 539–550, Apr. 1999.

[2] H. Kobayashi, M. Morimura, K. Kobayashi, and Y. Onaya, “Aperture Jitter Effects in Wideband ADC Systems,” in *Proc. 6th IEEE International Conference on Electronics, Circuits and Systems (ICECS ’99)*, Pafos, Cyprus, Sept. 1999, pp. 1705–1708.

[3] S. S. Awad, “Analysis of Accumulated Timing-Jitter in the Time Domain,” *IEEE Trans. Instrum. Meas.*, vol. 47, no. 1, pp. 69–73, Feb. 1998.

[4] A. Papoulis and S. U. Pillai, *Probability, Random Variables and Stochastic Processes*, 4th ed. McGraw-Hill Education, 2002.

[5] A. Demir, A. Mehrotra, and J. Roychowdhury, “Phase Noise in Oscillators : A Unifying Theory and Numerical Methods for Characterization,” *IEEE Trans. Circuits Syst. I*, vol. 47, no. 5, pp. 655–674, May 2000.

[6] G. Matz and F. Hlawatsch, “Time-varying power spectra of nonstationary random processes,” to appear in *Time-Frequency Signal Analysis and Processing*, B. Boashash, Ed., Englewood Cliffs (NJ): Prentice Hall, 2002.